Journal Pre-proof

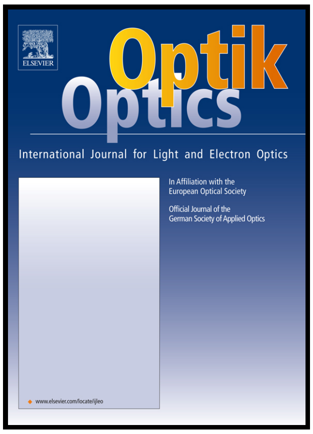

The effect of laser surface melting on the retained austenite and wear properties of AISI D2 tool steel

Amir Moradiani, Zeinab Malekshahi Beiranvand, R.M. Chandima Ratnayake, Amir Aliabadi, Mehdi Rasoulinia

PII: S0030-4026(21)01970-7

DOI: https://doi.org/10.1016/j.ijleo.2021.168469

Reference: IJLEO168469

To appear in: *Optik*

Received date: 22 October 2021
Accepted date: 8 December 2021

Please cite this article as: Amir Moradiani, Zeinab Malekshahi Beiranvand, R.M. Chandima Ratnayake, Amir Aliabadi and Mehdi Rasoulinia, The effect of laser surface melting on the retained austenite and wear properties of AISI D2 tool steel, *Optik,* (2021) doi:https://doi.org/10.1016/j.ijleo.2021.168469

The effect of laser surface melting on the retained austenite and wear properties of AISI D2 tool steel

Amir Moradiani*[1] Zeinab Malekshahi Beiranvand [2], R.M. Chandima Ratnayake [3], Amir Aliabadi[4], Mehdi Rasoulinia [5]

[1] Tarbiat Modares University, Department of Materials engineering, Tehran, Iran,
amir.moradiyan@gmail.com

[2] Tarbiat Modares University, Department of Materials engineering, Tehran, Iran,
z.malekshahi.beiranvand@gmail.com

[3] Stavanger University, Department of Mechanical and Structural Engineering and Materials Science, Stavanger, Norway,
chandima.ratnayake@uis.no

[4] Tehran University, School of Metallurgy and Materials Engineering, College of Engineering, Iran,
parsa.aliabadi.96@gmail.com

[5] Borujerd Azad Eslami University, Department of Engineering, Lorestan, Iran,
mehdi.rasoulinia@gmail.com

Corresponding Author:
Amir Moradiani
Tarbiat Modares University
Iran
Phone: +989355953074
Fax: not available
E-mail: amir.moradiyan@gmail.com

Abstract

In this study the effect of laser surface melting (LSM) on the amount of retained austenite, hardness and wear resistance of AISI D2 steel was investigated utilizing hardness test, X-ray diffraction (XRD), pin on disk wear test and scanning electron microscopy (SEM). In order to evaluate wear resistance, pin on disk tests at two different loads were carried out on surface treated samples including as received annealed and a quenched and tempered specimen. Surface treatment has been carried out in three different conditions; LSM, LSM with pre-heating at 300°C and LSM with pre-cooling in liquid nitrogen which resulted in 64, 42 and 90 percent of retained austenite respectively, revealing that higher cooling rate led to a higher amount of retained austenite. The results showed that in spite of the presence of austenite as major phase in re-melted surface, the hardness reached to the values of up to 600 HV_{10} which is approximately two times of the as received steel having a lot of carbides dispersed in the ferrite matrix. In addition, at lower load, conventionally heat treated sample exhibited better wear resistance, whereas at higher load, the wear rate of laser melted specimen was the least as a result of the transformation of retained austenite into martensite. At lower load the dominant wear mechanism was abrasion while Adhesion was identified as the main wear mechanism at higher load.

Key words: Laser surface melting, Retained austenite, Wear resistance, cold work tool steel

Introduction

High-carbon high-chromium tool steels are important engineering materials for producing cutting tools and cold forming dies. AISI D2 is the main alloy of this group which has the highest amount of alloying elements in cold work tool steels. These steels are subjected to high wear stresses in service, especially in deep drawing and extrusion applications [1, 2]. Therefore, various ways have been explored to improve their surface properties. Changing conventional heat treatment parameters[3], cryo-treatment and deep cryogenic treatments by liquid nitrogen [4-8],plasma nitriding [9], friction stir processing (FSP) [10], depositing a layer of TiN or TiAlN by means of plasma assisted physical vapor deposition(PAPVD) on the surface[11], modification of surface layers by laser heat treatment[12], and many other methods are examples of those attempts in order to improve the wear behavior and extend the tool lifespan. Surface melting by using energetic beams such as ion, electron, laser and plasma is one of the innovative approaches used to improve the surface characteristics.

Some research works have been carried out in order to investigate the effects of LSM on the microstructure and characteristics of tool steels. Yasavol et al. [13] exhibited an increase of 2-4 times in the micro hardness of the pulsed laser melted zone of AISI D2 steel. Spranger and Hilgenberg [14] improved surface characteristics of AISI D2 by conducting a surface texture via LSM and implantation of TiB2 particles. Zou et al. [15] investigated the phases in the surface layer of AISI D2 exposed to the high current pulsed electron beam. They reported that as a result of 10^7 K/s cooling rate, the martensitic phase and carbides disappeared and metastable and nanostructured fine austenite grains were formed. Nagaoka et al. [16] investigated the hardness and microstructure of a laser cladded layer of D2 tool steel and the changes occurred after FSP. They reached a maximum hardness of 857 Hv in that layer due to formation of fine M7C3 carbide particles and martensite. Bartkowska et al. [17] employed the combination of diffusion boronizing process and subsequent laser remelting to obtain higher surface characterestics in Vanadis-6 cold work tool steel. Morisada et al. [18] fabricated a nanostructured layer of D2 consisting of Nanoparticles of M7C3 carbides by combination of laser cladding and FSP. Sturm et al.[19]investigated the effect of pre-heating on the surface characteristics of a Vanadium-rich cold work tool steel during LSM. They reported a coarser microstructure in comparison with which typically evolves during the laser-melting, and a reduction in the volume fraction of retained austenite as a result of using pre-heating. The effect of retained austenite and dispersion of carbides on wear properties of laser treated alloy steels has been investigated by some researchers. Dilawary et al. [20] stated that LSM can have a detrimental effect on the wear resistance of plasma transfer arc deposited M2 high speed steel because of lower volume fractions of carbides and lower hardness. Colaco and Villar [21, 22] investigated a number of laser surface melted samples of 420 martensitic stainless steel with different content of retained austenite which are produced by changing laser parameters and concluded that as a result of the stress-induced transformation of austenite into martensite, the wear resistance of LSM specimens increased compared with that of the conventionally treated material.

The retained austenite can play a vital role in figuring out the wear resistance of steels. Some research demonstrated that the retained austenite can enhance wear resistance via its high ductility nature and transformation-induced plasticity (TRIP) effect. Indeed, the wear properties improve as a result of increasing the work hardening capacity of the material. In addition, internal compressive stresses induced by volume expansion stem from transformation of retained austenite to martensite hinder crack propagation [23-26]. However, in some cases detrimental effect of retained austenite on wear properties has been reported. In fact, the morphology, stability, distribution and amount of retained austenite are important factors in wear performance [24, 27].

To date, Research in the field of LSM in steels has focused more on the stainless steels and corrosion resistance of resulted structures [28], while LSM in tool steels can be considered as a solution to heal cracks developed during their use[29, 30], eliminate cracks and voids in repaired tools and also as a substitution of required heat treatment after repair welding which can contribute to serious heat treatment cracks in large expensive dies and molds [31-33]. And this will be possible only if the laser surface melted steel exhibits wear properties at least equal to the heat-treated steel. Therefore, it is indispensable to study the wear properties of tool steels after laser surface melting. Despite a number of investigations being carried out, so far, few studies have been carried out to investigate the effect of laser melting on the amount of retained austenite and its effect on the wear behavior in cold work tool steels. Furthermore, the role of retained austenite on wear performance in these steels is not yet fully comprehended. Stabilization of austenite and removal of chromium carbides is more important in high carbon high chromium tool steels because they derive all their wear properties from carbides. This paper aims to clarify the changes in microstructure and phases of AISI D2 tool steel melted by Nd: YAG pulsed laser, effects of pre-heating and precooling and the role of the amount of retained austenite in the wear behavior of this alloy.

In present study, the cooling rate in solidification of remelted zone was controlled by applying preheating and precooling; the amount of retained austenite in resulted structures was precisely determined and in-depth investigation of wear properties of laser surface melted zone with focus on the behavior of retained austenite in different situations has carried out.

Methodology

Laser surface melting was performed with 3 different conditions leading to dissimilar cooling rates. As-processed workpieces were investigated by XRD analysis and the amount of retained austenite was calculated. A pin on disk wear test with 2 different loads was carried out and wear test results of laser surface melted samples and conventionally heat treated samples were compared.

Experimental details

A machined disk with 5mm thickness was used in the present study. The chemical composition is shown in table 1. The surface of samples was ground, polished, and cleaned with acetone before laser treatment.

Table 1- Chemical Composition of Steel

C	Si	S	P	Mn	Cr	Mo	V
1.6	0.27	0.001	0.023	0.34	11.4	0.81	0.91

A Nd:YAG pulsed laser apparatus with a mean power of 400w was employed to re-melt the steel surface. Argon flows at 30 l/min used as the shielding gas. The distance between the specimen and laser source was adjusted by 2mm to optimize the depth of the re-melted area.

Laser parameters were set according to table 2. The melted surface was produced by 35% overlapping ratio of single tracks.

Table2-Pulsed Laser Operating Parameters

Pulse Wide (ms)	Energy (J)	Mean Power (W)	Peak Power (KW)	Scanning velocity(mm/s)	Overlapping (%)	Lateral Overlapping (%)
5	8	160	1.6	6.7	67	35

Surface melting of specimens carried out under three different condition which are shown schematically in fig. 1. First specimen, preheated laser surface melted (PHLSM), was preheated to 300 °C in an electric furnace and a heater under the specimen was used to maintain temperature during the process. Another sample laser surface melted (LSM) without any pre cooling or preheating process. The third one, precooled laser surface melted (PCLSM), was precooled at -196 °C by emerging in liquid nitrogen for 15 minutes. In order to maintain the temperature during the laser processing, a sealed ceramic container with a copper sheet on top were employed which was filled up with dry ice and the sample was located directly on the copper sheet. Therefore, continuous heat transfer occurred during laser treatment. The surface temperature controlled by a thermometer during the process and when it reached to -50^{0}C, the specimen and container returned into the liquid nitrogen. Characteristics of these samples were compared to a quenched tempered (QT) sample which was heat-treated by austenizing at 1050 °C, quenching in oil and double tempering at 450 °C.

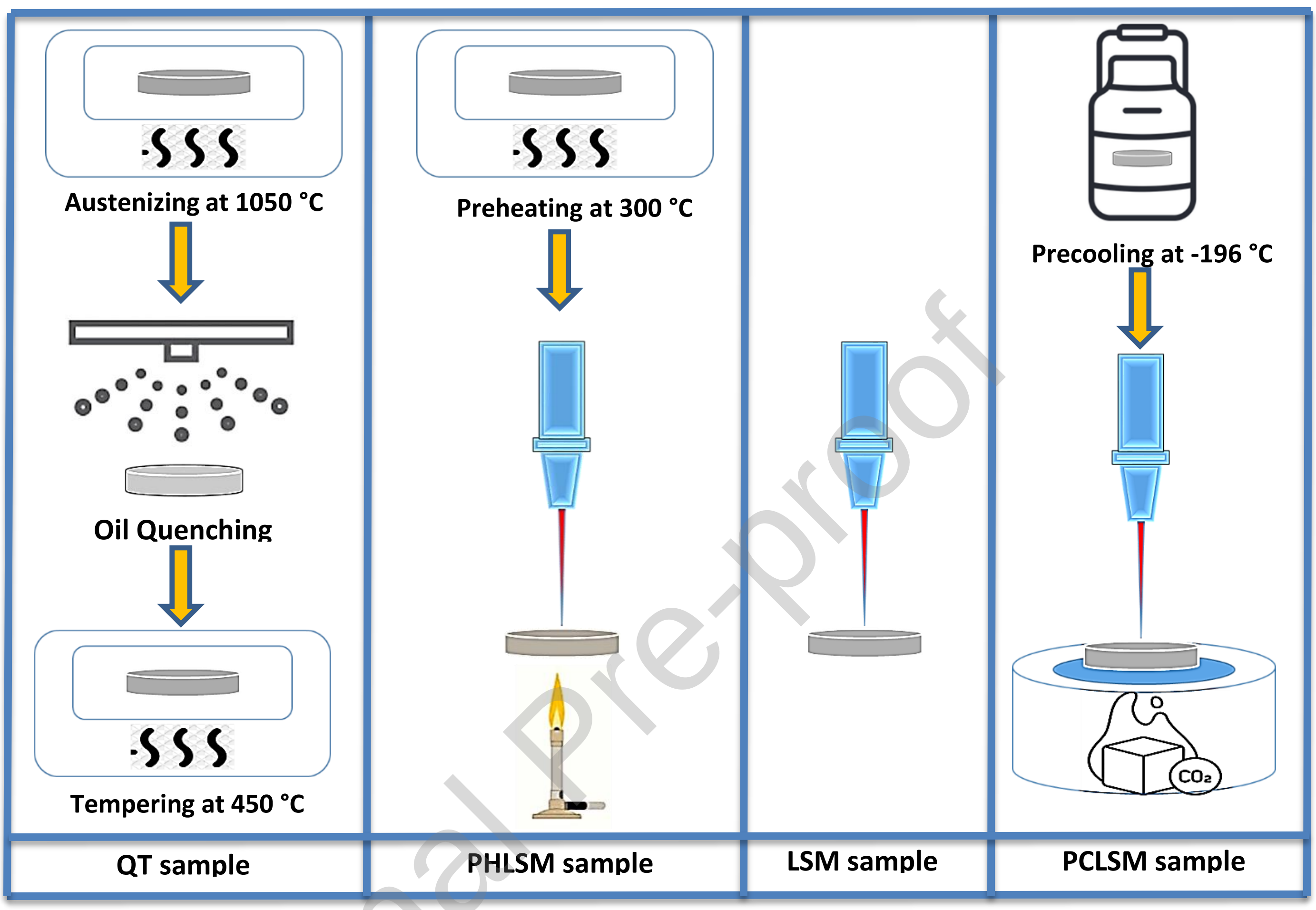

Fig. 1. Schematic diagram of different samples

Cross section of treated samples was investigated using optical microscopy, scanning electron microscopy (SEM model: TESCAN, WEGA2), and electro etching to evaluate the microstructural changes. Micro hardness was measured by a Vickers hardness tester, according to ASTM E384-03. Applied load was 500g and remained for 15 seconds. Reported hardness numbers are the mean of 3 measured data on polished surfaces of laser treated specimens.

In addition, to investigate the phase changes before and after laser melting, XRD Analyses with Cu Kα irradiation were carried out on a (Philips-X'PERT, MPD) device. The amount of retained austenite is estimated according to the ASTM E975-03 standard. This standard can be used to determine retained austenite in steels up to 15 percent alloying element and D2 tool steel yield about 14 percent of alloying elements. In this method the volume fraction of austenite is calculated by using the intensity of both austenite and martensite (or ferrite) peaks in XRD patterns.

$$V_y = \left[\frac{\left(\frac{1}{q}\sum_{j=1}^{q}\frac{I_{\gamma j}}{R_{\gamma j}}\right)}{\left(\frac{1}{q}\sum_{j=1}^{q}\frac{I_{\gamma j}}{R_{\gamma j}}\right)+\left(\frac{1}{P}\sum_{i=1}^{P}\frac{I_{\alpha i}}{R_{\alpha i}}\right)}\right] \qquad (1)$$

I_γ and $I\alpha$ are the intensity of martensite and austenite peaks and R is a scale factor which depends on Bragg angle, crystal structure and multiplicity and structure factor of each plane.

In this study diffraction properties of three planes (111), (200) and (220) of austenite phase and three planes (110), (211) and (200) of ferrite/martensite phase were used to calculate the amount of retained austenite.

Wear testing was carried out on a pin on disk machine with two different loads. The test specimen is prepared as a pin with a 6mm diameter by a wire-cut EDM which is shown in Fig. 2. The disk was made of alumina with about 1500 Hv. Condition of wear test is shown in table 3.

Table 3- wear test condition

Disc Diameter	Total Distance	Linear Velocity	Load
14 Cm	1000 m	5 Cm/s	20 N- 40 N

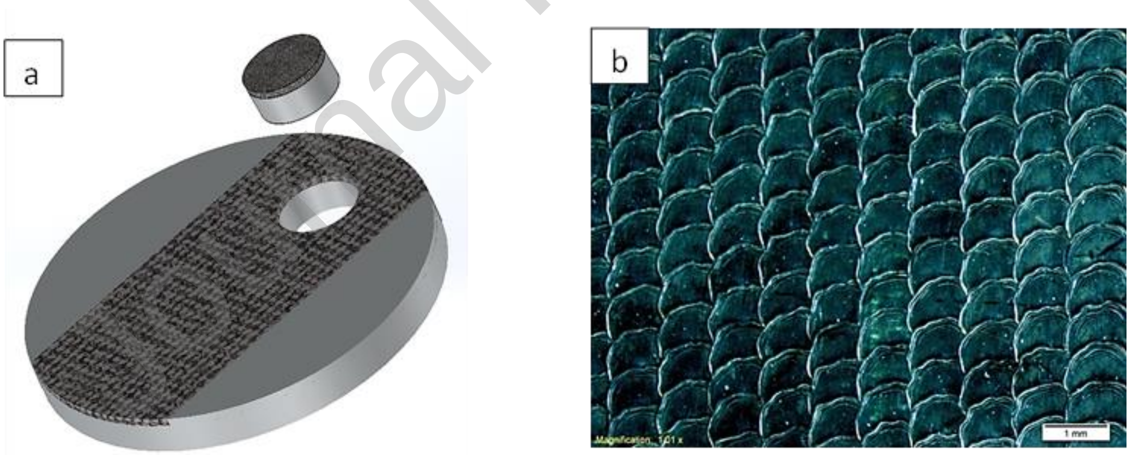

Fig. 2. a) Laser surface melted zone and the pin which is cut by Wire-cut EDM to use in wear test b) microscopic image of laser surface melted which is made by overlapping of single pulses

Results and discussions

Microstructure of heat treated AISI D2 steel was formed of a tempered martensite with the dispersion of coarse primary carbides and finer secondary carbides. In surface re-melted samples, as shown in Fig. 3, the microstructure of melted areas was almost fully dendritic with no chromium carbide particles found in the matrix. It seems fine dendrites were epitaxially grown from the fusion line toward the center of melted area, due to high compositional under cooling, related to the high amount of alloying elements and high solidification rate [34, 35].

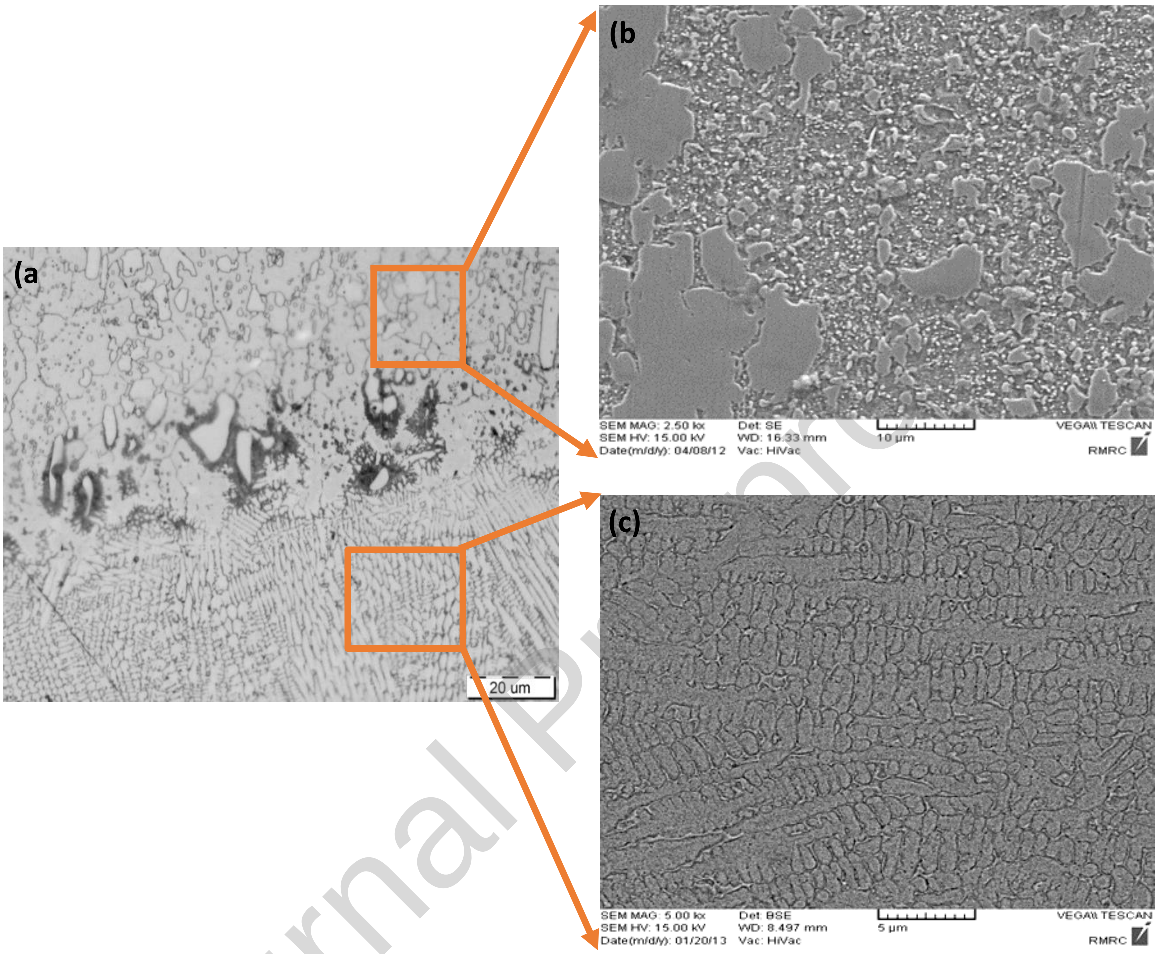

Fig. 3. Structural changes after laser surface remelting a) OM image of QT base metal and melt pool b) SEM image of dendritic Structure in remelted zone c) SEM image of dispersion of carbides in QTbase metal

Fig. 4 shows the X-ray diffraction patterns for different samples. From the analysis of these patterns, QT steel includes martensite, chromium carbides and some retained austenite. The carbide peaks disappeared in the XRD pattern of re-melted surfaces and there was only a very low intensity M_7C_3 peak in PHLSM sample. In these specimens, dominant phase was clearly retained austenite. The intensity of Austenite peak of A (200) rapidly increased in precooled sample.

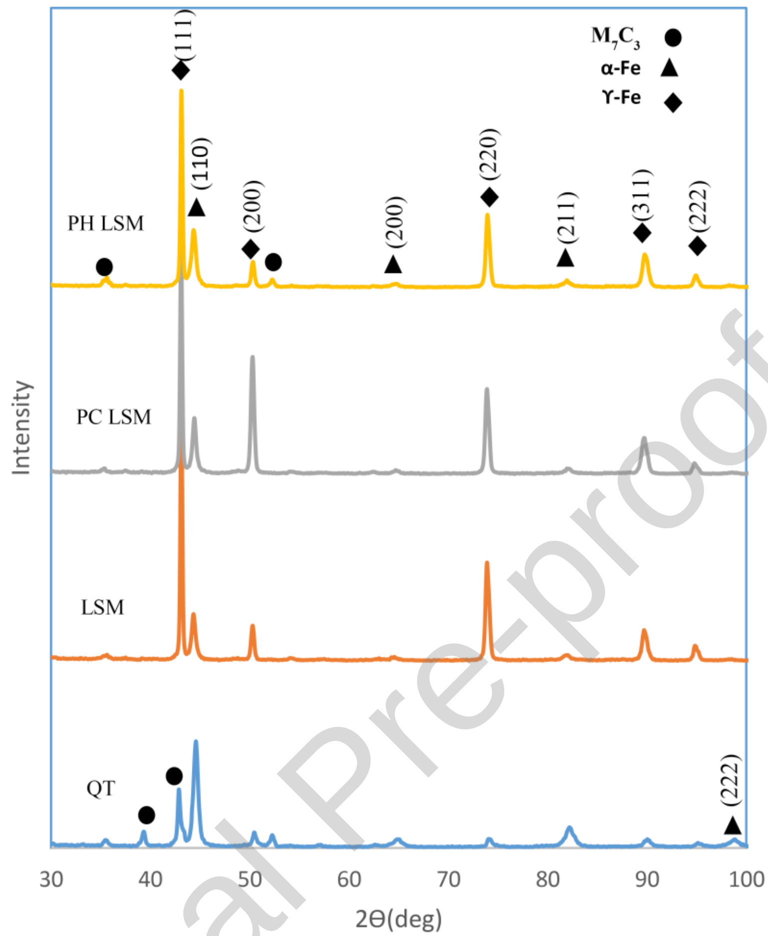

Fig. 4. X-ray diffraction patterns

Austenite was stabilized in the laser melted area because of the rapid solidification condition. As a result of high cooling rate through solidification after laser surface melting, shear strength of austenite increases and temperature start of martensite decreases. Therefore, the higher cooling rate results in a higher amount of retained austenite [22, 36]. In addition, Since there are a high amount of alloying elements in D2 tool steel such as carbon, chromium and vanadium, the supersaturation of alloying elements in austenite can be considered as another key factor for increasing the strength against martensitic deformation [21, 22]. Furthermore, severe residual stresses in subsurface and high density of dislocations in melt pool are considered as reasons of stabilization of non-equilibrium phases in laser surface remelting [22, 37].

Table 4 shows the estimated amount of retained austenite in 3 different conditions of the laser melted area. It is obvious that with increasing the cooling rate in the melted zone by precooling, the amount of austenite increased to 90 percent. In preheated specimen, the amount of retained austenite is lowest at 42 percent due to lower cooling rate in comparison with LSM specimen which have 64 percent of austenite.

Table 4- retained austenite in different laser treated samples.

Sample	LSM	PHLSM	PCLSM
Percent of Retained austenite	64	42	90

Fig. 5 shows the hardness of the base metal, QT specimen and LSM specimens. These results showed that both QT and LSM lead to an increase in surface hardness. The hardness of the D2 steel in the annealing condition was 310HV. The QT specimen had the maximum hardness equal to 620HV. High hardness value in this sample were directly related to the higher volume friction of hard carbides of Cr_7C_3 in the microstructure.[38] Although the presence of retained austenite in melted layer caused lower hardness in comparison to QT sample, the hardness of laser treated samples was much higher than that of annealed specimen. PCLSM had the least hardness among laser treated samples at 470HV while the PHLSM sample was hardest at 580HV. The results of hardness were compatible with the percentage of retained austenite so that the more retained austenite led to less hardness. It was considerable that for all three samples, the hardness was higher than general hardness of the austenite phase; it can be related to super saturation and high distortion in the austenite matrix. Besides, very fine dendritic structure could be another reason for higher hardness of re-melted samples in comparison to common hardness of this phase.[39]

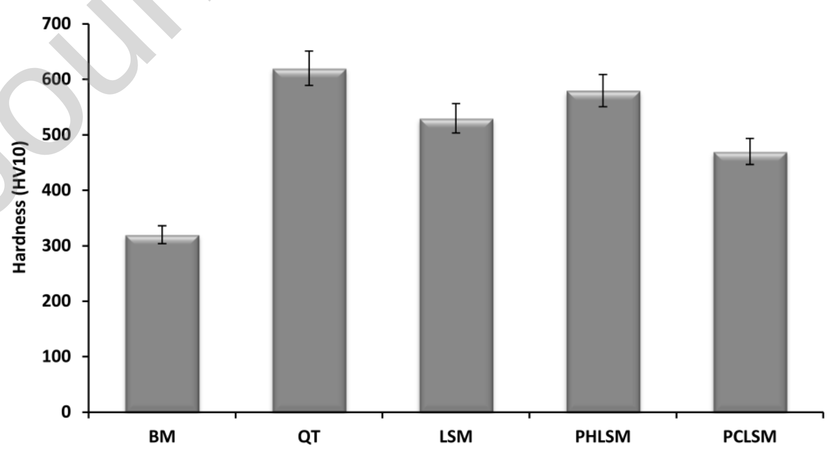

Fig. 5. hardness of different samples

The wear rate of annealed, quenched-tempered and laser surface melted samples at different applied wear loads are plotted in Fig. 6. Firstly, it can be concluded that surface melting reduced the wear rate to three times lower than that of the as received annealed steel. Moreover, the results indicated that the QT sample showed less wear rate compared to the laser treated samples at 20N load while LSM sample showed better wear resistance than others at the applied load of 40N indicating the role of residual austenite in the wear behavior of surface melted steels.

Although the QT sample showed less wear rate compared to the laser treated samples at 20N load, the results indicated that wear rate was approximately 1.5 times at higher load 40N as compared to that of 20N. It is well known that higher hardness leads to less real contact area between sliding surfaces which results in wear rate reduction according to Archard's wear equation (Eq. 2)[3, 40]. So, the higher wear resistance of QT over laser treated samples with less hardness was not unexpected. Moreover, the rise in wear rate due to the increase in force is justified by this equation. But the surprising point is that the wear rate of LSM and PHLSM samples has decreased by the rise in applied load.

$$w \propto \frac{W}{H} \tag{2}$$

Where w is wear rate, W is the total load and H is surface hardness of wearing material.

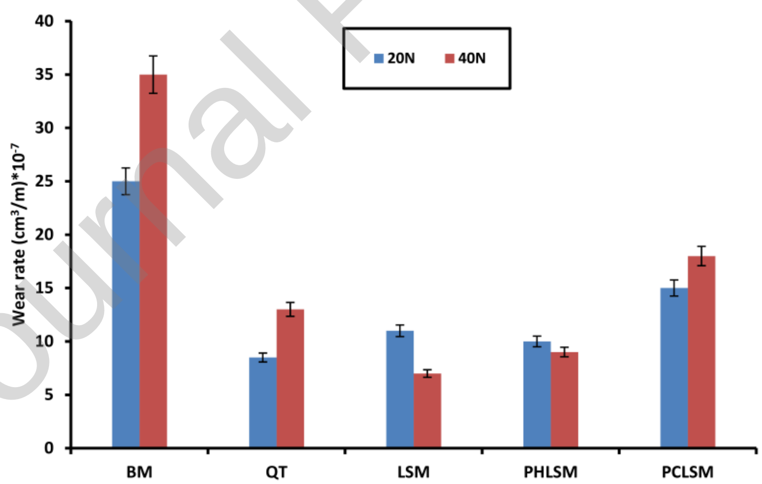

Fig. 6. The wear rate of base metal (BM), QT, LSM, PHLSM, and PCLSM specimens at loads of 20N and 40N.

Pervious investigations on the wear behavior of D2 steel had shown that the main factors can affect the wear behavior is hardness, microstructure and especially retained austenite [3]

X-ray diffraction patterns before and after the wear test of LSM sample is shown in Fig. 7. According to this pattern, the retained austenite reflections reduced after the wear tests. This is more evident at higher force and implies that almost all the near surface retained austenite has transformed into martensite during the wear process under an applied load of 40N.

Microstructure evolution and phase transformation are known as the major factors for work hardening of the steels with high amount of retained austenite and are more likely to occur under higher applying loads.[25, 41]

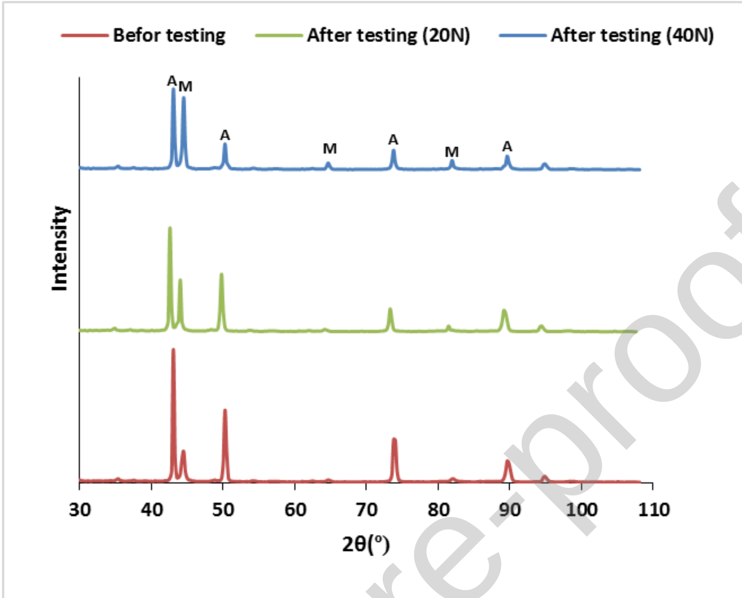

Fig. 7. XRD pattern of LSM sample worn surface.

The worn surfaces of the QT sample at two applied loads are given in Fig. 8. Due to the high surface hardness of this sample, during wear at an applied load of 20N, the surface was less affected and only a few small scratches were observed on it. Increasing the applied load to 40N led to an increase in the surface stress, consequently, the wear rate has increased and it is also consistent with the literature on wear of martensitic tool steels.[3] The dominant wear mechanism at both loads was abrasion. Moreover, at the higher load there was some evidence of oxide detachment at the worn surface.

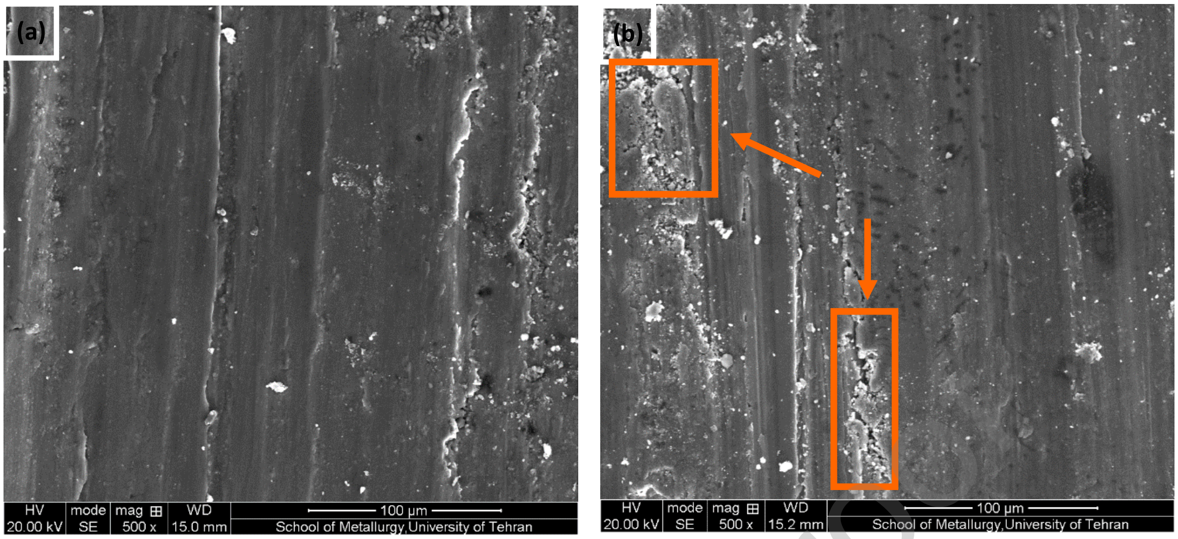

Fig. 8. SEM micrograph of worn surface of QT sample in the applying load of (a) 20N and (b) 40N.

At the lower load (20 N), the PHSLM sample showed the best wear resistance among laser treated samples. However, the PCLSM exhibited the highest mass loss. Fig. 9a and 9b show worn surfaces of these two samples at 20N applied load. Abrasion scratches and indications of detachment areas were evident on the surface of PHSLM sample. While, ploughing mechanism seems to be predominant in PCLSM. The PHLSM had the lowest retained austenite (42%) and consequently the highest hardness than the other surface melted samples and therefore, it also showed the highest wear resistance in the applied load of 20N. The XRD pattern of surface detachments related to PHLSM sample at applying load of 20N is also shown in Fig. 10 exhibiting sharp peaks of the oxides. The EDS analysis of debris of worn surface of PHLSM sample given in Fig. 11 indicating high percentage of oxygen in these zones too. Therefore, it can be concluded that the detachment on the worn surface of PHLSM sample has been created due to the formation and breaking of oxides. During the sliding motion, the frictional energy is dissipated as heat. As a consequence of frictional heating, surface oxidation can occur and thus oxidized patches can form on the wear scar. Oxidative type of wear is one of the wear mechanisms in PHLSM sample which can be attributed to higher hardness and presence of carbides in comparison to other laser treated samples. Higher amount of carbides in tool steels can lead to predominance of oxidative type of wear[42].

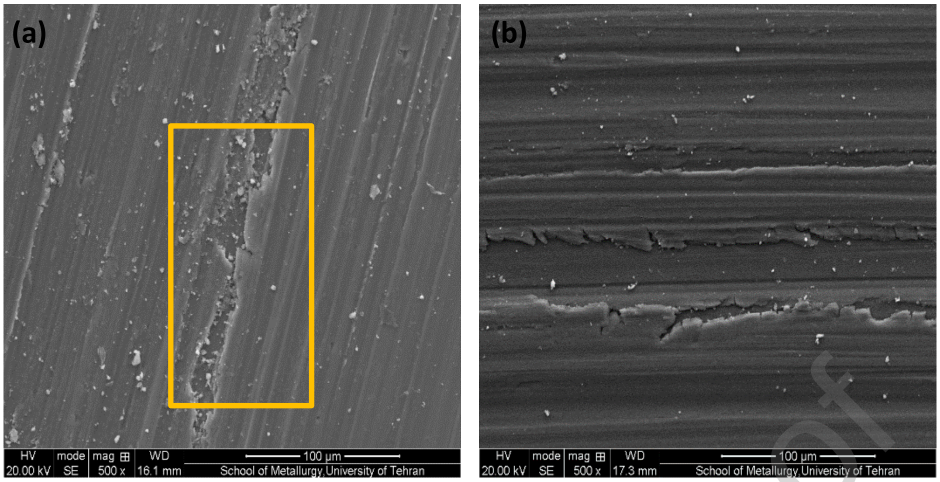

Fig. 9. SEM micrograph of worn surface of (a) PHSLM and (b) PCSLM samples in the applying load of 20N.

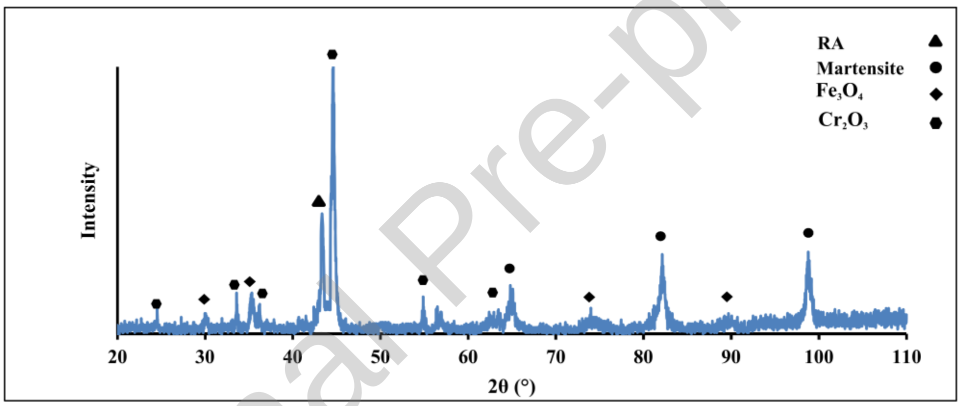

Fig. 10. XRD Analysis of PHLSM worn surface at applied load of 40N

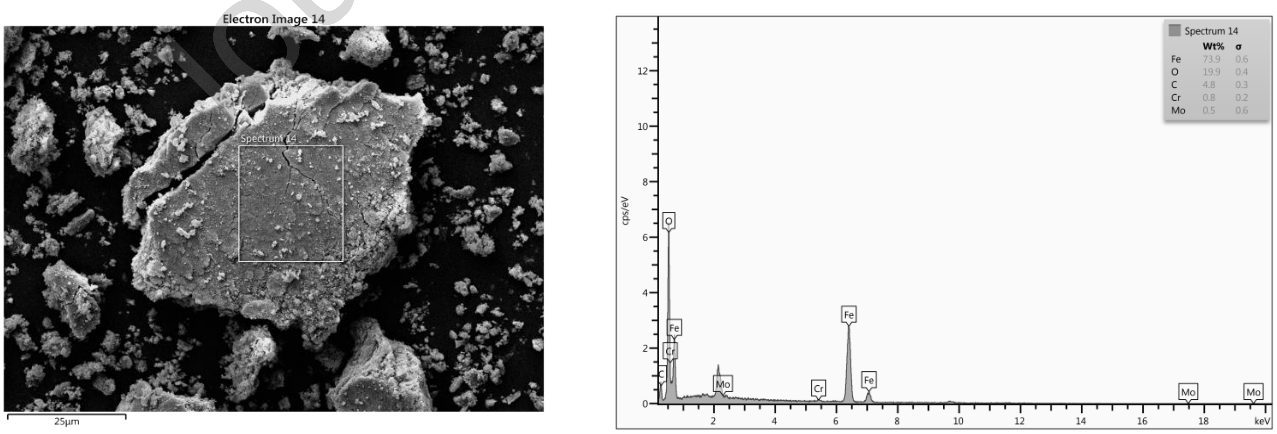

Fig. 11. EDS analyses of PHLSM wear debris.

Fig. 12(a) and 12(b) show worn surfaces of LSM and PCLSM samples in the applied load of 40N. Worn surface of the LSM sample at the wear load of 40N was comparatively smooth with no sharp edges. Because under abrasive conditions, plastic deformation usually occurs in the soft region with retained austenite component which leads to phase transformation of retained austenite, and the mechanically induced martensite formation contributes to the strengthening effect on the worn surface [25, 41]. Moreover, it was reported that the morphology, stability and amount of retained austenite can have a profound impact on wear performance [3, 27, 38, 41, 43] Worn surface of PCLSM steel was relatively rough and abrasive craters are most commonly observed. As mentioned before, PCLSM had the highest retained austenite in the microstructure so during the wear process under a high applied load; the hardened areas tend to undertake much more strain fatigue wear, while the comparatively soft areas tend to undertake much more ploughing-cutting wear. High loading leads to ploughing-cutting and then the formation of grinding triturate on the worn surface. As a result, the ploughing cutting morphology is preserved on the worn surface.

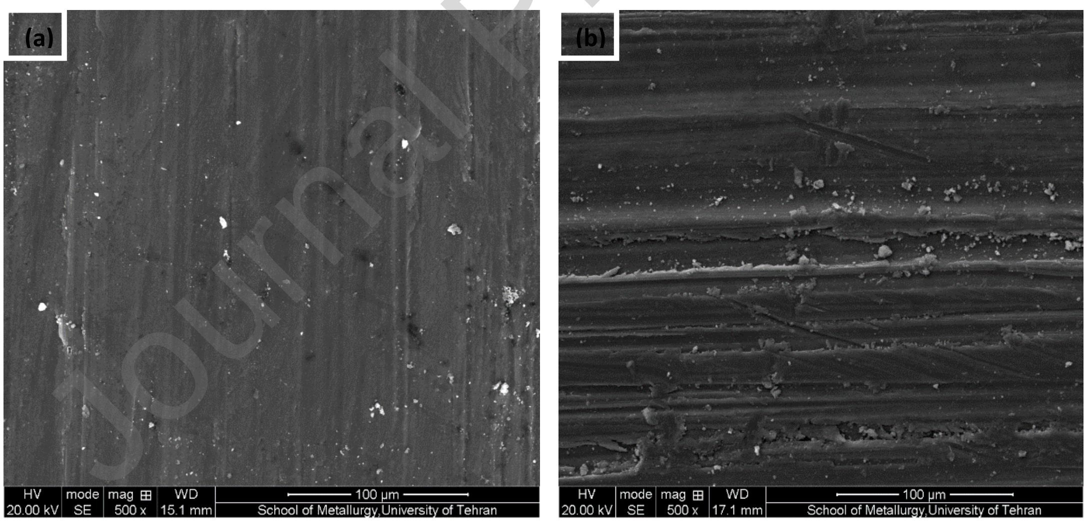

Fig. 12. SEM micrograph of worn surface of (a) LSM and (b) PCSLM samples in the applying load of 40N.

SEM micrographs of the worn specimen cross-sections in Fig. 13 indicate the microstructural changes under the worn surfaces. Fig. 13 shows no tribo-layers on the worn surface and therefore, cross section can be divided into two different distinct zones. Zone 1 is intact material. Zone 2 is located at the top of the cross section and underwent plastic deformation. As can be seen in Fig. 13, the microstructure alignment in zone 2 is parallel to the sliding direction and in the areas close to the contact surface, the deformation is more pronounced.

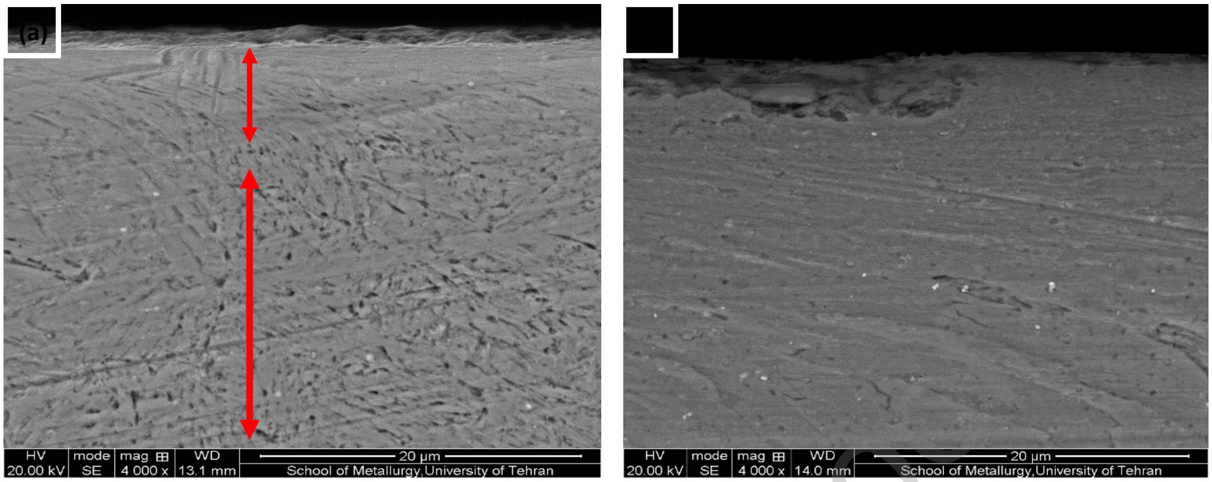

Fig. 13. SEM micrographs of the worn specimen cross-sections of (a) LSM sample and (b) PCLSM sample

Cross sectional micro hardness profile of the SLM and PCLSM samples at the applied load of 40N is shown in Fig.14. Micro-hardness variation curves indicated surface hardening for both steels, however, depth of the affected layer is about 25 µm for LSM samples and nearly 50 µm for PCLSM samples. This can explain why the LSM sample showed better wear resistance. The PCLSM sample showed lower strength and hardness based on the rather soft single austenite phase. Therefore, plastic deformation had easily gone into deeper layers of surface treated zones, the wear force distributed in wider areas and less strain induced martensite had formed. However, LSM with 64% of retained austenite had higher strength properties and showed higher strain hardening ability in a narrower affected layer.

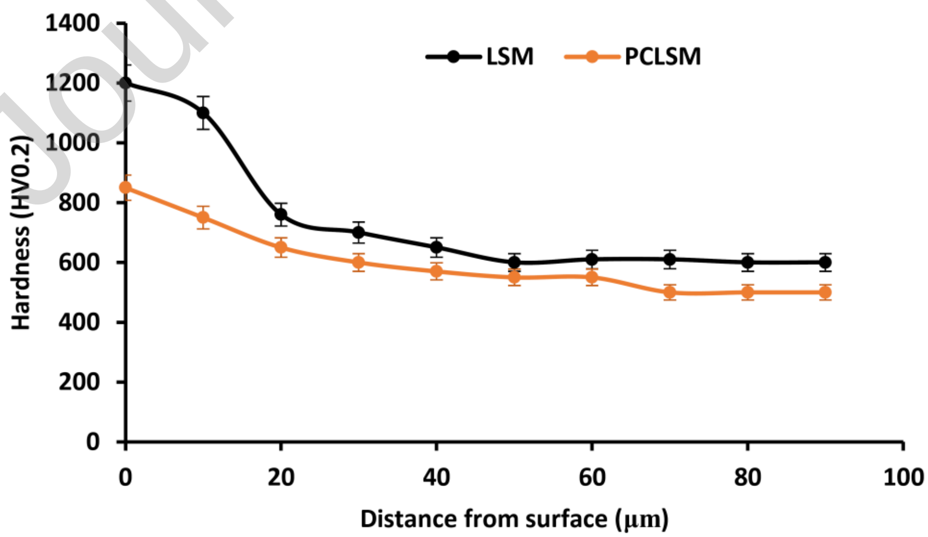

Fig. 14. Hardness profile from the worn surface of LSM and PCLSM samples.

Conclusion

The dry sliding wear behavior of the laser surface melted of D2 steel in three conditions including LSM, LSM with pre-heating (PHLSM), and LSM with pre-cooling (PCLSM) was investigated and compared with that of the conventional quench tempered steel. The conclusions from this work are:

1. Re-melting the surface with a pulsed laser resulted in stabilization of retained Austenite in a dendritic structure. The LSM sample contained 64% of retained austenite. The amount of retained austenite soared to 90% with increasing the cooling rate in PCLSM while it dropped to 42% in PHLSM.
2. In laser treated samples, the retained austenite underwent strain induced transformation, resulting in formation of martensite under wear test conditions. It was more observable at the higher wear load. The newly formed martensite contributed to the formation of a hardened layer on the worn surface, causing the wear to slow down.
3. The wear resistance of all surface melted samples outperformed the quenched and tempered sample in high applied loads. Wear resistance improved by a factor of two with 64% retained austenite in the microstructure compared to conventional heat-treated QT samples.
4. LSM sample with 64% of retained austenite exhibited better wear resistance under higher load conditions over against PHLSM & PCLSM sample as a result of optimum retained austenite in the microstructure which led to high work hardening capacity in a narrow surface layer.
5. In the PCLSM sample with 90% retained austenite and lowest hardness among all samples, a ploughing mechanism and deeper zone of plastic deformation led to the highest rate of wear in both applied loads.
6. In addition to microstructure, surface oxidation played a prominent role in determining the wear resistance. During the wear process, an oxidative type of wear mechanism occurred for the PHLSM and QT sample and oxidized patches formed on the surface. It can be attributed to higher relative hardness and presence of carbides in these samples.

Future Studies:

Present study investigated the role of retained austenite in wear properties of laser surface melted AISI D2 tool steel and it was shown that although fully austenitic microstructure is not desirable, a high amount of retained austenite in laser melted zone can exhibit high wear resistance. Since laser operational parameters such as energy and pulse width directly affects the cooling rate, future studies could fruitfully explore this issue further by using Design of Experiments (DoE) to find out optimal laser parameters that provides best wear properties based on findings of this research.

Research Ethics

We further confirm that any aspect of the work covered in this manuscript that has involved human patients has been conducted with the ethical approval of all relevant bodies and that such approvals are acknowledged within the manuscript.

References

1. Tang, L., et al., *Dry sliding friction and wear behaviour of hardened AISI D2 tool steel with different hardness levels.* Tribology International, 2013. **66**: p. 165-173.
2. Cora, Ö.N. and M. Koç, *Experimental investigations on wear resistance characteristics of alternative die materials for stamping of advanced high-strength steels (AHSS).* International Journal of Machine Tools and Manufacture, 2009. **49**(12): p. 897-905.
3. Singh, K., R.K. Khatirkar, and S.G. Sapate, *Microstructure evolution and abrasive wear behavior of D2 steel.* Wear, 2015. **328-329**: p. 206-216.
4. Podgornik, B., et al., *Deep cryogenic treatment of tool steels.* Journal of Materials Processing Technology, 2016. **229**: p. 398-406.
5. Ghasemi-Nanesa, H. and M. Jahazi, *Simultaneous enhancement of strength and ductility in cryogenically treated AISI D2 tool steel.* Materials Science and Engineering: A, 2014. **598**: p. 413-419.
6. Amini, K., A. Akhbarizadeh, and S. Javadpour, *Effect of deep cryogenic treatment on the formation of nano-sized carbides and the wear behavior of D2 tool steel.* International Journal of Minerals, Metallurgy, and Materials, 2012. **19**(9): p. 795-799.
7. Das, D., A.K. Dutta, and K.K. Ray, *Correlation of microstructure with wear behaviour of deep cryogenically treated AISI D2 steel.* Wear, 2009. **267**(9): p. 1371-1380.
8. Akhbarizadeh, A., A. Shafyei, and M.A. Golozar, *Effects of cryogenic treatment on wear behavior of D6 tool steel.* Materials & Design, 2009. **30**(8): p. 3259-3264.
9. TobołA, D., et al., *Structure and Properties of Burnished and Nitrided AISI D2 Tool Steel.* Materials Science, 2015. **21**(4).
10. Yasavol, N. and A. Ramalho, *Wear properties of friction stir processed AISI D2 tool steel.* Tribology International, 2015. **91**: p. 177-183.
11. Staia, M.H., et al., *Hardness properties and high-temperature wear behavior of nitrided AISI D2 tool steel, prior and after PAPVD coating.* Wear, 2009. **267**(9-10): p. 1452-1461.

12. Lesyk, D.A., et al., *Microstructure related enhancement in wear resistance of tool steel AISI D2 by applying laser heat treatment followed by ultrasonic impact treatment.* Surface and Coatings Technology, 2017. **328**: p. 344-354.
13. Yasavol, N., et al., *Microstructure and mechanical behavior of pulsed laser surface melted AISI D2 cold work tool steel.* Applied Surface Science, 2013. **265**: p. 653-662.
14. Spranger, F. and K. Hilgenberg, *Dispersion behavior of TiB2 particles in AISI D2 tool steel surfaces during pulsed laser dispersing and their influence on material properties.* Applied Surface Science, 2019. **467-468**: p. 493-504.
15. Zou, J., et al., *Microstructures and phase formations in the surface layer of an AISI D2 steel treated with pulsed electron beam.* Journal of Alloys and Compounds, 2007. **434**: p. 707-709.
16. Nagaoka, T., et al., *Friction stir processing of a D2 tool steel layer fabricated by laser cladding.* Materials & Design, 2015. **83**: p. 224-229.
17. Bartkowska, A., et al., *Microstructure, microhardness, phase analysis and chemical composition of laser remelted FeB-Fe2B surface layers produced on Vanadis-6 steel.* Optics & Laser Technology, 2016. **86**: p. 115-125.
18. Morisada, Y., et al., *Fabrication of nanostructured tool steel layer by combination of laser cladding and friction stir processing.* Surface and Coatings Technology, 2011. **205**(11): p. 3397-3403.
19. Šturm, R., M. Štefanikova, and D. Steiner Petrovič, *Influence of pre-heating on the surface modification of powder-metallurgy processed cold-work tool steel during laser surface melting.* Applied Surface Science, 2015. **325**: p. 203-210.
20. Dilawary, S.A.A., et al., *Modification of M2 hardfacing: Effect of molybdenum alloying and laser surface melting on microstructure and wear performance.* Wear, 2018. **404**: p. 111-121.
21. Colaço, R. and R. Vilar, *On the influence of retained austenite in the abrasive wear behaviour of a laser surface melted tool steel.* Wear, 2005. **258**(1-4): p. 225-231.
22. Colaço, R. and R. Vilar, *Stabilisation of retained austenite in laser surface melted tool steels.* Materials Science and Engineering: A, 2004. **385**(1-2): p. 123-127.
23. Sourmail, T., et al., *Evaluation of potential of high Si high C steel nanostructured bainite for wear and fatigue applications.* Materials Science and Technology, 2013. **29**(10): p. 1166-1173.
24. Moghaddam, P.V., et al., *Effect of retained austenite on adhesion-dominated wear of nanostructured carbide-free bainitic steel.* Tribology International, 2020. **150**: p. 106348.
25. Moghaddam, P.V., et al., *The role of retained austenite in dry rolling/sliding wear of nanostructured carbide-free bainitic steels.* Wear, 2019. **428-429**: p. 193-204.
26. Leiro, A., et al., *Wear of nano-structured carbide-free bainitic steels under dry rolling–sliding conditions.* Wear, 2013. **298-299**: p. 42-47.
27. Wang, Y., R. Song, and L. Huang, *The effect of retained austenite on the wear mechanism of bainitic ductile iron under impact load.* Journal of Materials Research and Technology, 2021. **11**: p. 1665-1671.
28. Khalfallah, I.Y., et al., *Microstructure and corrosion behavior of austenitic stainless steel treated with laser.* Optics & Laser Technology, 2011. **43**(4): p. 806-813.

29. Cabeza, M., et al., *Laser surface melting: A suitable technique to repair damaged surfaces made in 14 Ni (200 grade) maraging steel.* Surface and Coatings Technology, 2012. **212**: p. 159-168.
30. Nikam, S.H. and N.K. Jain, *Laser-based repair of damaged dies, molds, and gears*, in *Advanced Manufacturing Technologies*. 2017, Springer. p. 137-159.
31. Šolić, S., B. Podgornik, and V. Leskovšek, *The occurrence of quenching cracks in high-carbon tool steel depending on the austenitizing temperature.* Engineering Failure Analysis, 2018. **92**: p. 140-148.
32. Siddiqui, A.A. and A.K. Dubey, *Recent trends in laser cladding and surface alloying.* Optics & Laser Technology, 2021. **134**: p. 106619.
33. Jhavar, S., C.P. Paul, and N.K. Jain, *Causes of failure and repairing options for dies and molds: A review.* Engineering Failure Analysis, 2013. **34**: p. 519-535.
34. Pleterski, M., et al., *Laser Cladding of Cold-Work Tool Steel by Pulse Shaping.* Journal of Materials Science & Technology, 2011. **27**(8): p. 707-713.
35. Grosdidier, T., et al., *Grain refinement, hardening and metastable phase formation by high current pulsed electron beam (HCPEB) treatment under heating and melting modes.* Journal of Alloys and Compounds, 2010. **504, Supplement 1**(0): p. S508-S511.
36. Kwok, C.T., et al., *Microstructural and corrosion characteristics of laser surface-melted plastics mold steels.* Materials Science and Engineering: A, 2003. **357**(1–2): p. 94-103.
37. Colaço, R., C. Pina, and R. Vilar, *Influence of the processing conditions on the abrasive wear behaviour of a laser surface melted tool steel.* Scripta Materialia, 1999. **41**(7): p. 715-721.
38. Das, D., A.K. Dutta, and K.K. Ray, *Sub-zero treatments of AISI D2 steel: Part II. Wear behavior.* Materials Science and Engineering: A, 2010. **527**(9): p. 2194-2206.
39. Liu, W., N. Yan, and H. Wang, *Dendritic morphology evolution and microhardness enhancement of rapidly solidified Ni-based superalloys.* Science China Technological Sciences, 2019. **62**(11): p. 1976-1986.
40. Hutchings, I.M., *Tribology: friction and wear of engineering materials*. 1992: Butterworth-Heinemann Ltd.
41. Lu, J., et al., *Study of microstructure, mechanical properties and impact-abrasive wear behavior of medium-carbon steel treated by quenching and partitioning (Q&P) process.* Wear, 2018. **414-415**: p. 21-30.
42. Iakovakis, E., et al., *Evaluation of wear mechanisms in additive manufactured carbide-rich tool steels.* Wear, 2020. **462-463**: p. 203449.
43. Leiro, A., et al., *Tribological behaviour of carbide-free bainitic steel under dry rolling/sliding conditions.* Wear, 2011. **273**(1): p. 2-8.